

How mathematical AI is transforming biosciences

Guo-Wei Wei

Mathematics

Michigan State University

<http://www.math.msu.edu/~wei>



Home Programs ▾

Mathematical and Computational Biology
 Jun 12 - 16, 2023

Research partnerships:



Grant support: NIH, NSF, NASA, Pfizer, BMS, MEDC, Georgetown U, COVID-19 HPC Consortium, MSU Foundation, and MSU iCER



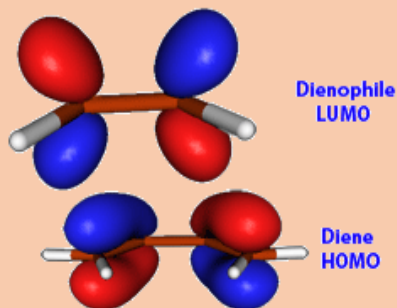
Four paradigms of scientific research

1st Paradigm:
Empirical
sciences



Experiments

2nd Paradigm:
Model-based
theoretical
sciences

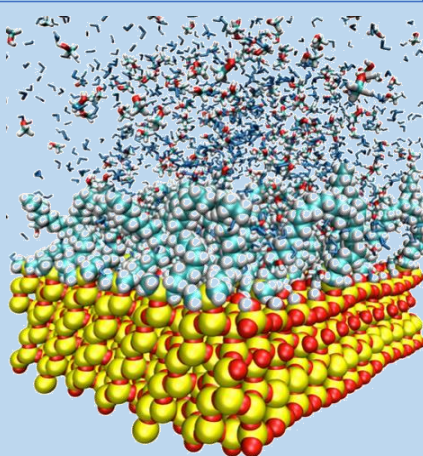


Math/Phys
models

1600

1950

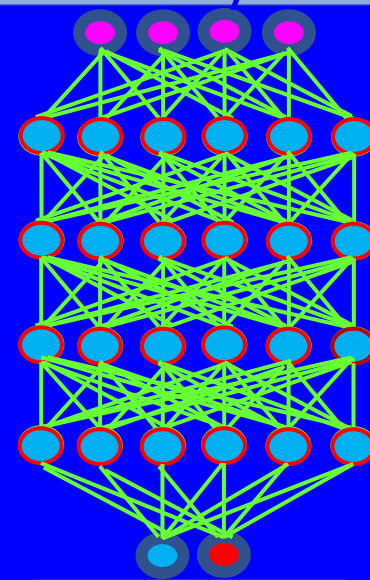
3rd Paradigm:
Computational
sciences



Computing,
simulation,
algorithms

2000

4th Paradigm:
Data-driven
scientific
discovery

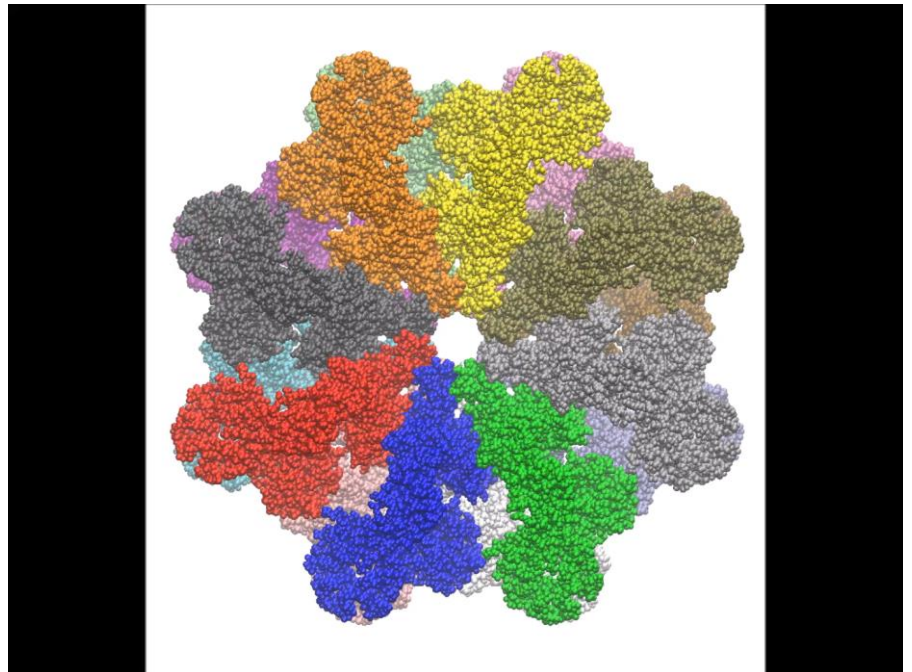
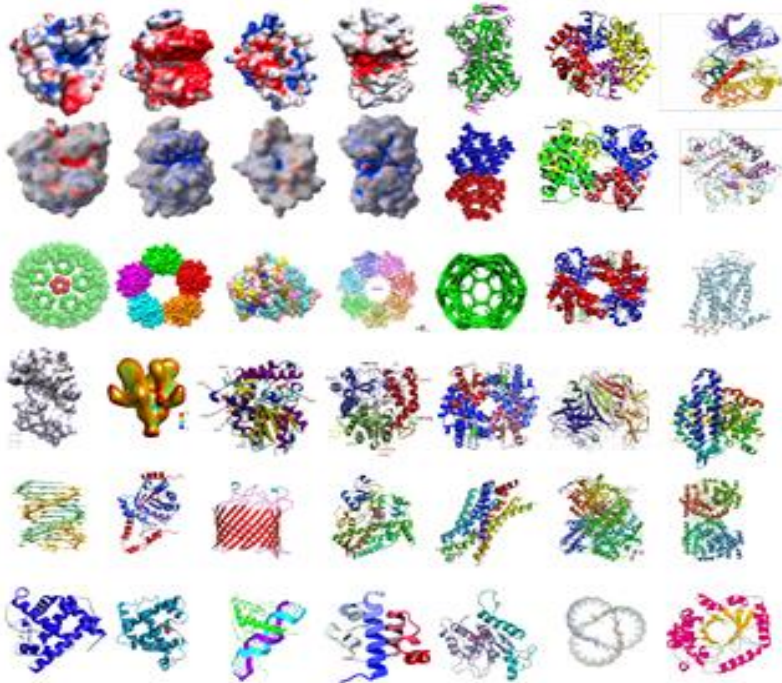


AI, machine
learning,
data science



Challenges of AI in biomolecular systems

- **Geometric dimensionality:** \mathbb{R}^{3N} , where $N \sim 5000$ for a protein.
- **Machine learning dimensionality:** $> 1024^3 m$, where m is the number of atom types in a protein.
- **Non-scalability: different sizes.**
- **Complexity:** intermolecular & intramolecular interactions.



Two schools of thinking

Given a protein with N atoms and an average of n electrons in each atom

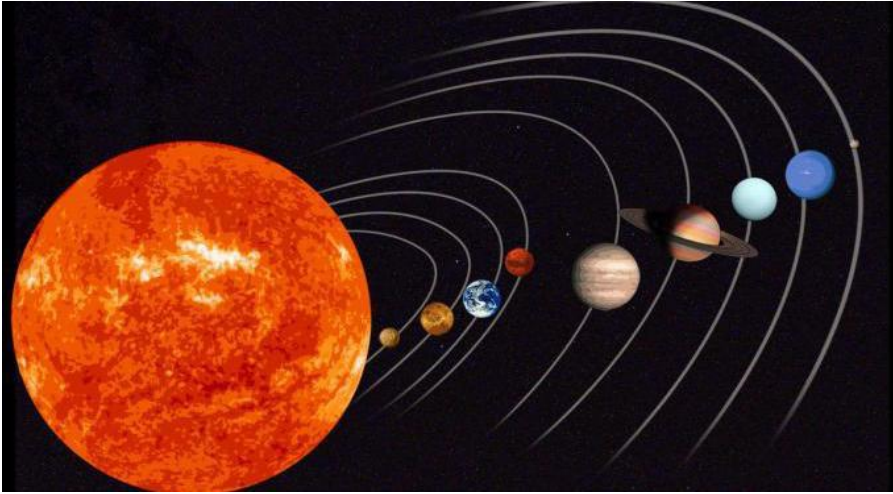
Fundamentalism; Mechanistic

Quantum Mechanics
 \mathbb{R}^{3Nn+3N}

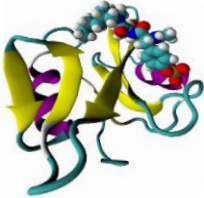
QM/MM \mathbb{R}^K
 $3N < K < 3N(n+1)$

Molecular Mechanics
 \mathbb{R}^{3N}

Multiscale Coarse-grain
 \mathbb{R}^M ($3 < M < 3N$)



Poisson-Boltzmann, PNP, etc. \mathbb{R}^3



Differentiable Manifold
 \mathbb{R}^2

Algebraic Topology
 \mathbb{R}^1

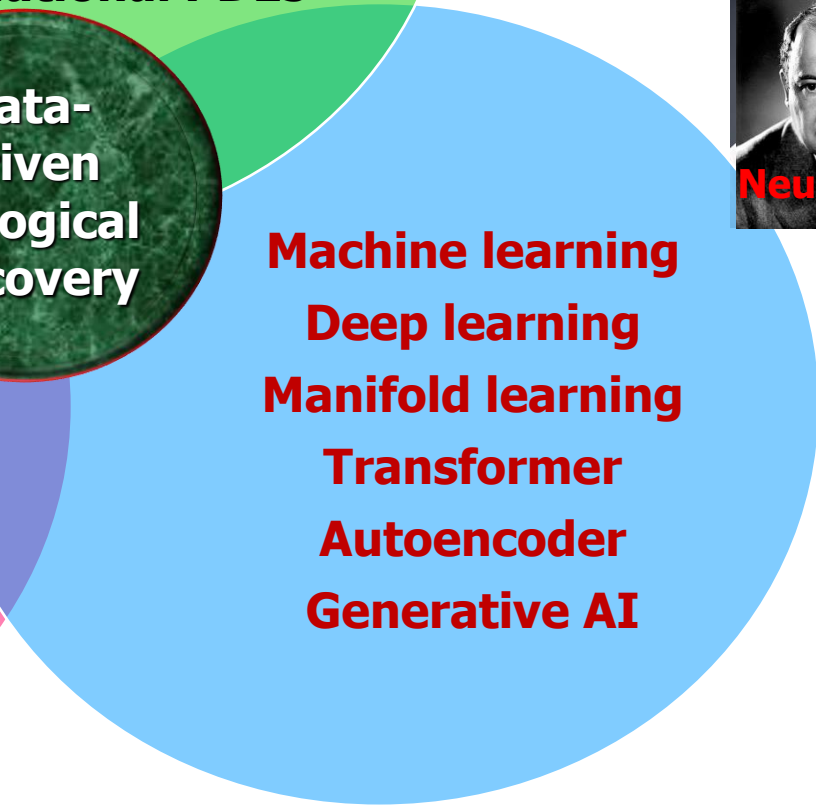
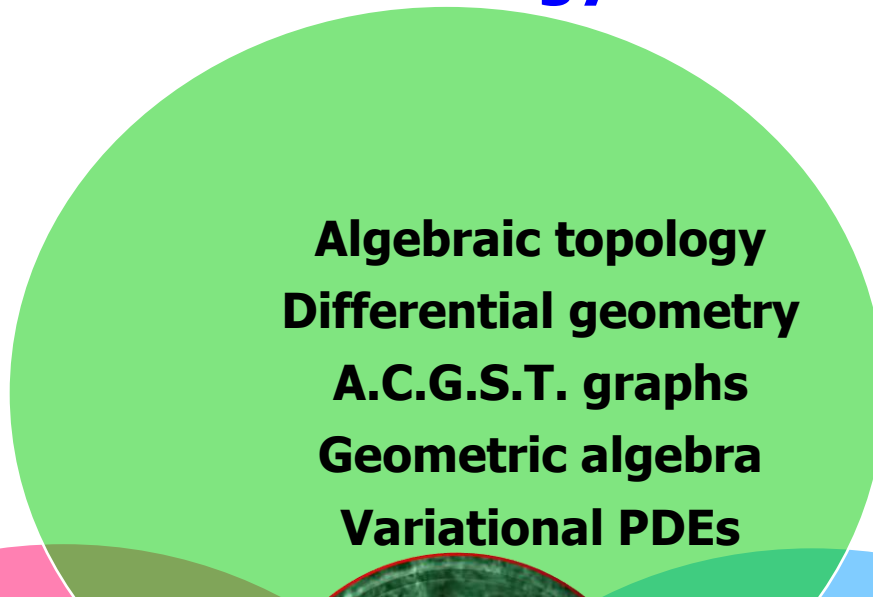
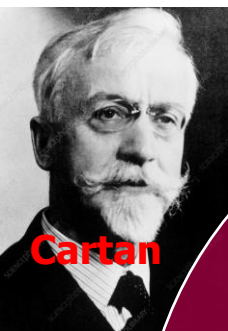
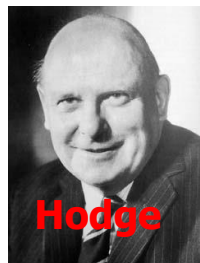
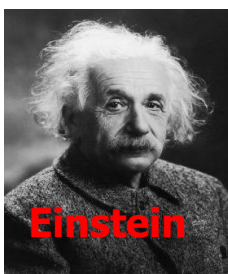
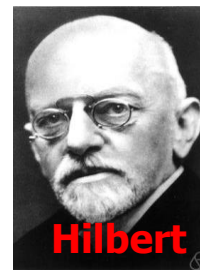
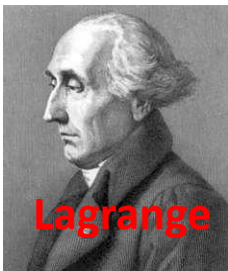
Basic hypothesis:
Intrinsic physics lies on low-dimensional manifolds in a high dimensional space

Reductionism; Data-driven

Graph Theory
 \mathbb{R}^0

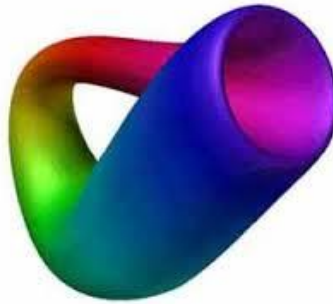
Index Theory
 \mathbb{R}^0

Our Strategy



Topology

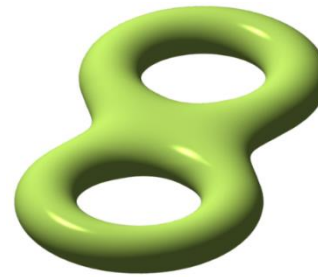
Klein Bottle (1882)



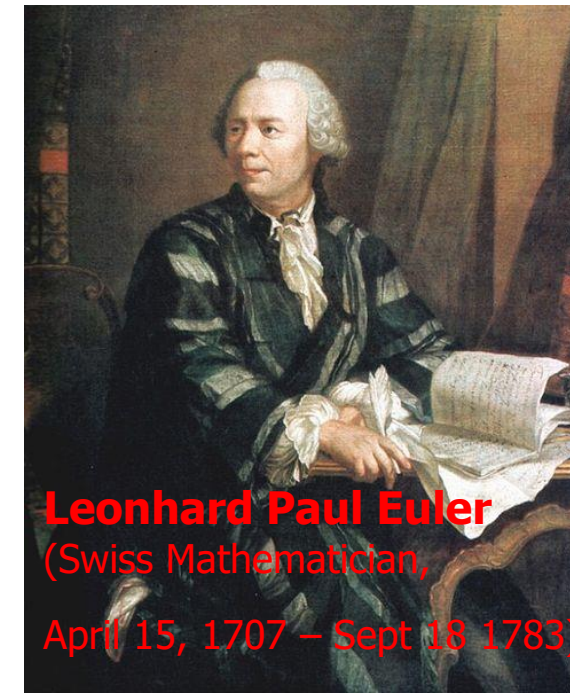
Torus



Double Torus

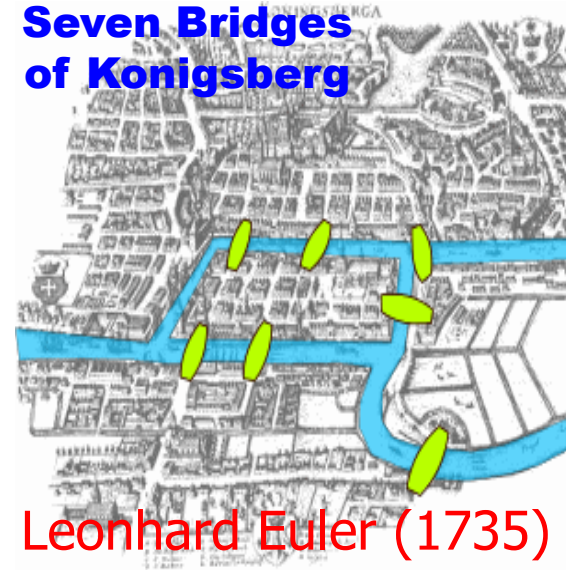


Augustin-Louis Cauchy,
Ludwig Schläfli,
Johann Benedict Listing,
Bernhard Riemann, and
Enrico Betti



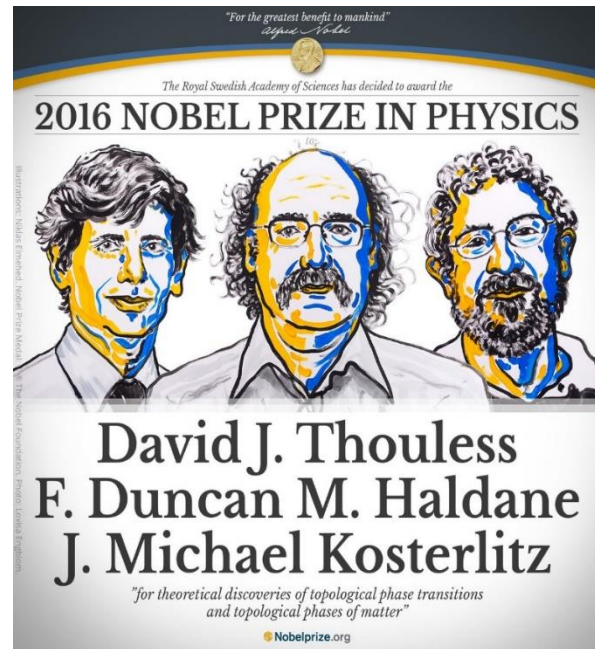
Leonhard Paul Euler
(Swiss Mathematician,
April 15, 1707 – Sept 18 1783)

**Seven Bridges
of Königsberg**



Leonhard Euler (1735)

Möbius Strips (1858)



Topological invariants: Betti numbers

β_0 is the number of connected components.

β_1 is the number of tunnels or circles.

β_2 is the number of cavities or voids.

Point

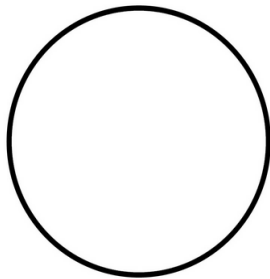


$$\beta_0 = 1$$

$$\beta_1 = 0$$

$$\beta_2 = 0$$

Circle

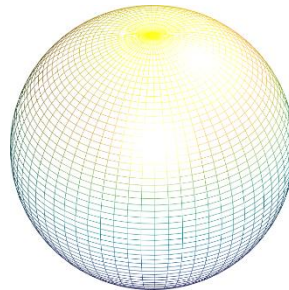


$$\beta_0 = 1$$

$$\beta_1 = 1$$

$$\beta_2 = 0$$

Sphere

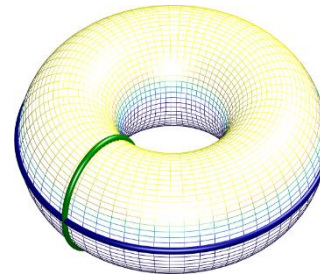


$$\beta_0 = 1$$

$$\beta_1 = 0$$

$$\beta_2 = 1$$

Torus



$$\beta_0 = 1$$

$$\beta_1 = 2$$

$$\beta_2 = 1$$

Limitation



L. Vieira



Crane and Segerman

Persistent homology induced by filtration

Simplexes:



0-simplex 1-simplex 2-simplex 3-simplex

k-chain: $K = \left\{ \sum_j c_j \sigma_j^k \right\}$

Chain group: $C_q(K, \mathbb{Z}_2)$

Boundary operator:

$$\partial_q \sigma^q = \sum_{j=0}^q (-1)^j \{v_0, v_1, \dots, \hat{v}_j, \dots, v_k\}$$

Cycle group: $Z_q = \text{Ker } \partial_q$

Boundary group: $B_q = \text{Im } \partial_{q+1}$

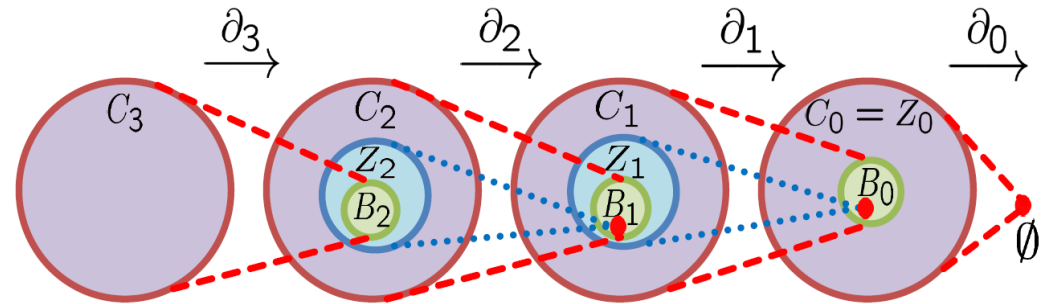
Homology group: $H_q = Z_q / B_q$

Betti number: $\beta_q = \text{Rank}(H_q)$

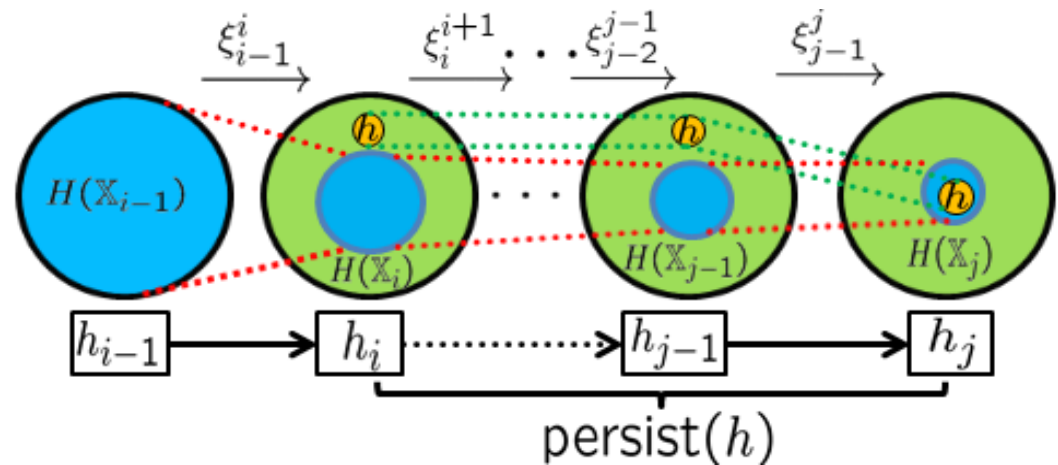
Xia, Wei, IJNMBE, 2014;

Xia, Feng, Tong, Wei, JCC, 2015

Frosini and Nandi (1999), Robins (1999), Edelsbrunner, Letscher and Zomorodian (2002), Zomorodian and Carlsson (2005), Edelsbrunner and Harer, (2007) Kaczynski, Mischaikow and Mrozek (2004), Ghrist (2008), ...

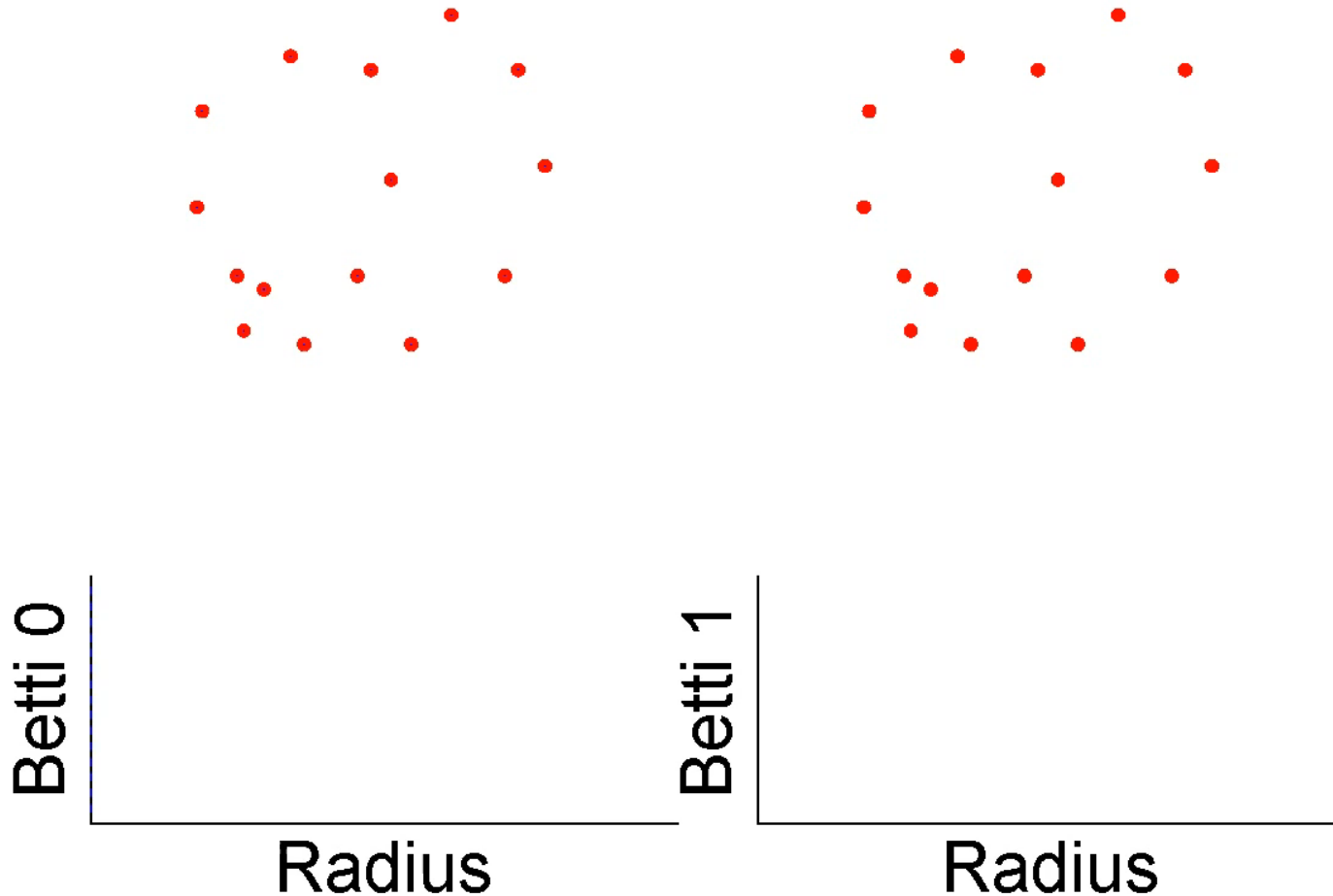


Filtration:

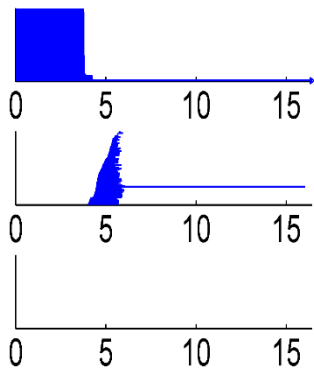
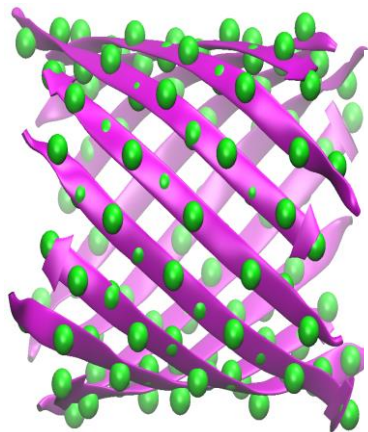
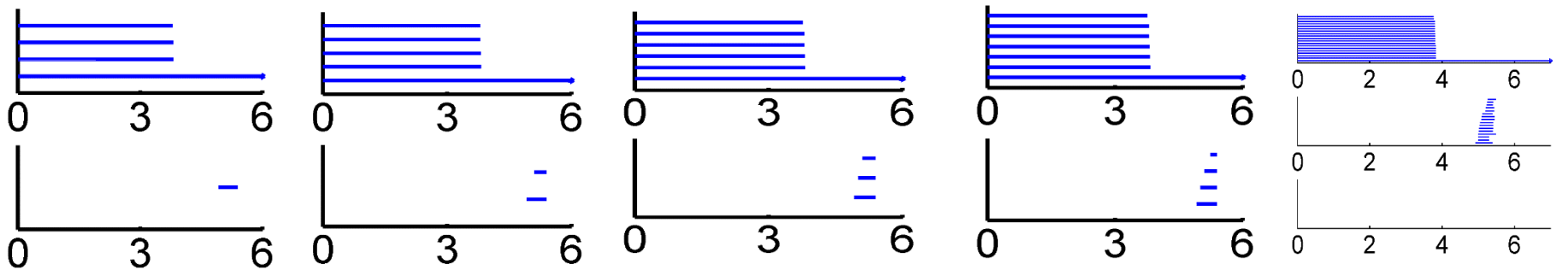
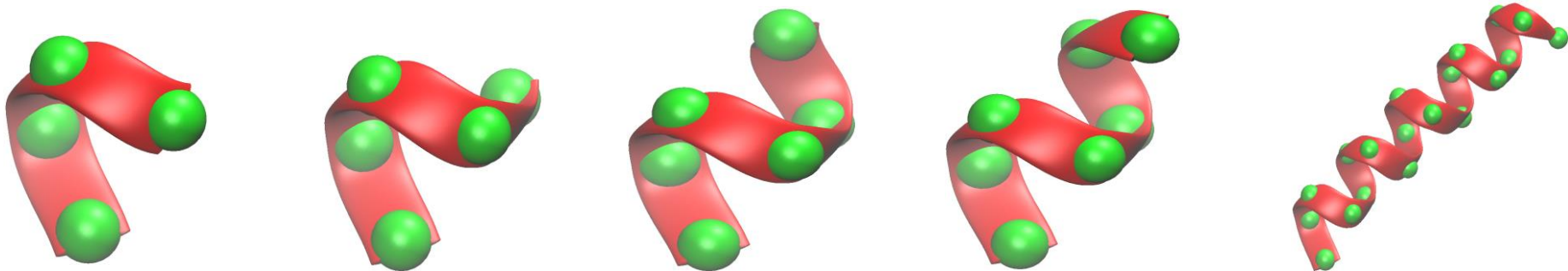


Topological data analysis

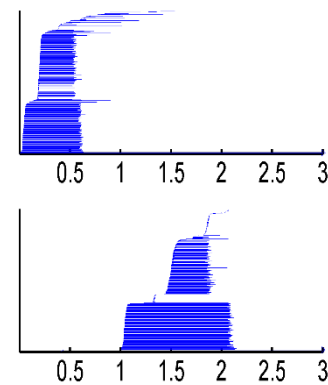
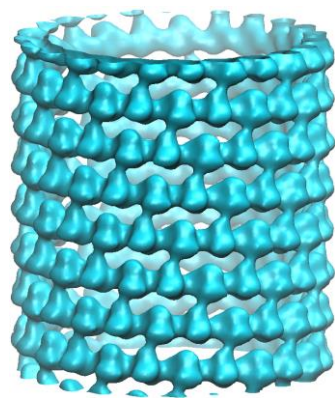
Vietoris-Rips complexes, **persistent homology** and **topological fingerprint** (Xia, Wei, 2014)



Topological fingerprints of an alpha helix, beta barrel, etc.



Beta barrel



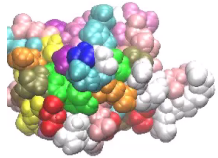
Microtubule



**(Xia & Wei,
IJNMBE,
2014, 2015)**

Topological data analysis

2D persistent homology of protein unfolding (1UBQ)



$$\mathbb{R}^{3N+1} \rightarrow \mathbb{R}^2$$

Radius



Kelin Xia

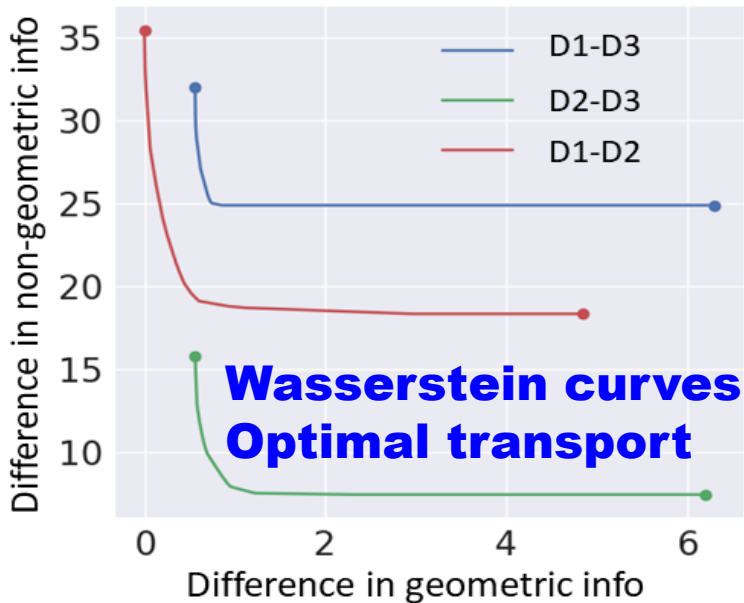
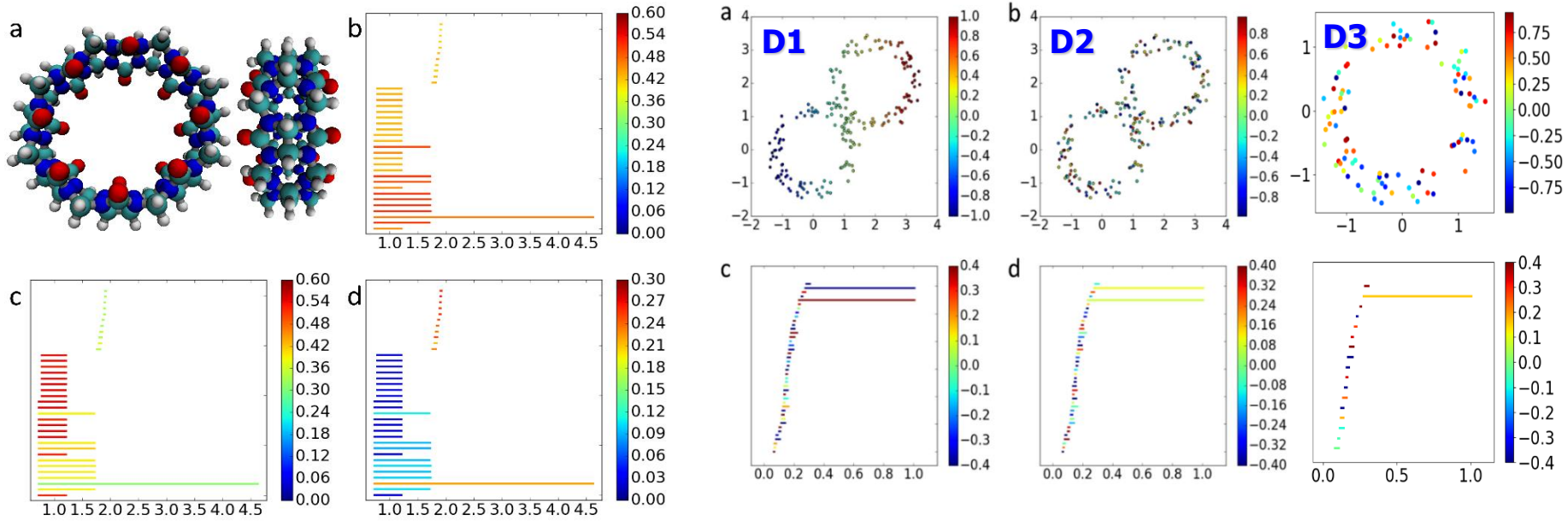
(Xia & Wei, JCC, 2015)

Limitations of persistent homology that prevent it from working well for many data

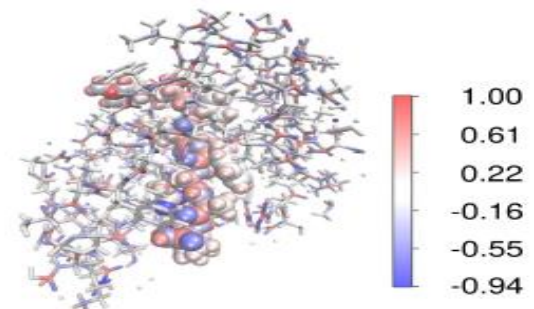
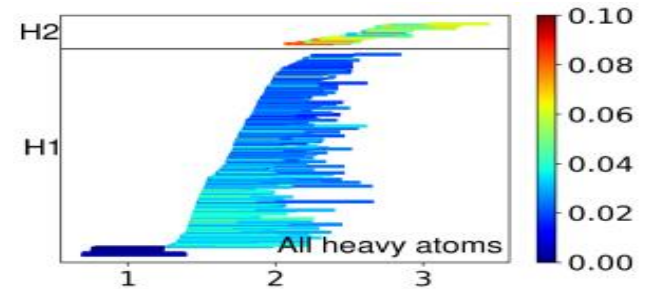
- It cannot handle heterogeneous information (i.e., different type of objects in the data)
- It is qualitative rather than quantitative (e.g., a 5-member ring is counted the same as a 6-member ring)
- It cannot describe non-topological changes (i.e., homotopic shape evolution over filtration)
- It is incapable of dealing with directed networks and digraphs (polarization, regulation, control issues)
- It is unable to characterize structured data (e.g., hypergraphs, directed networks)

We address these limitations with new topological methods

Persistent cohomology for heterogeneous data



Zixuan Cang
And Wei, SIAM
JMDS 2020



Combinatorial Graph (topological Laplacian)

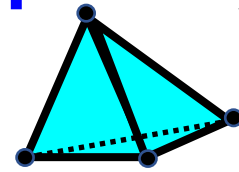
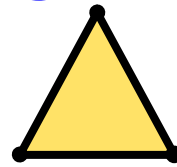
- Simplexes (σ^q):

0-simplex

1-simplex

2-simplex

3-simplex



- K -chain: $K = \left\{ \sum_j w_j \sigma_j^q \right\}$

(Eckmann 1944; Goldberg 2002; Horak, Jost, AIM, 2013; Serrano, Gomze, 2019,...)

- Chain group: $C_q(K, \mathbb{Z}_2)$

- Boundary operator: $\partial_q: C_q(K) \rightarrow C_{q-1}(K)$

$$\partial_q \sigma^q = \sum_{j=0}^q (-1)^j \{v_0, v_1, \dots, \hat{v}_j, \dots, v_q\}$$

- Adjoint boundary operator: $\partial_q^*: C_{q-1}(K) \rightarrow C_q(K)$

- q -combinatorial Laplacian operator: $\Delta_q = \partial_{q+1} \partial_{q+1}^* + \partial_q^* \partial_q$

- q -combinatorial Laplacian matrix: $\mathcal{L}_q = \mathcal{B}_{q+1} \mathcal{B}_{q+1}^T + \mathcal{B}_q^T \mathcal{B}_q$

- Betti numbers:

$$\beta_q = \dim(\mathcal{L}_q(K)) - \text{rank}(\mathcal{L}_q(K)) = \# \text{ of zero eigenvalues of } \mathcal{L}_q(K)$$

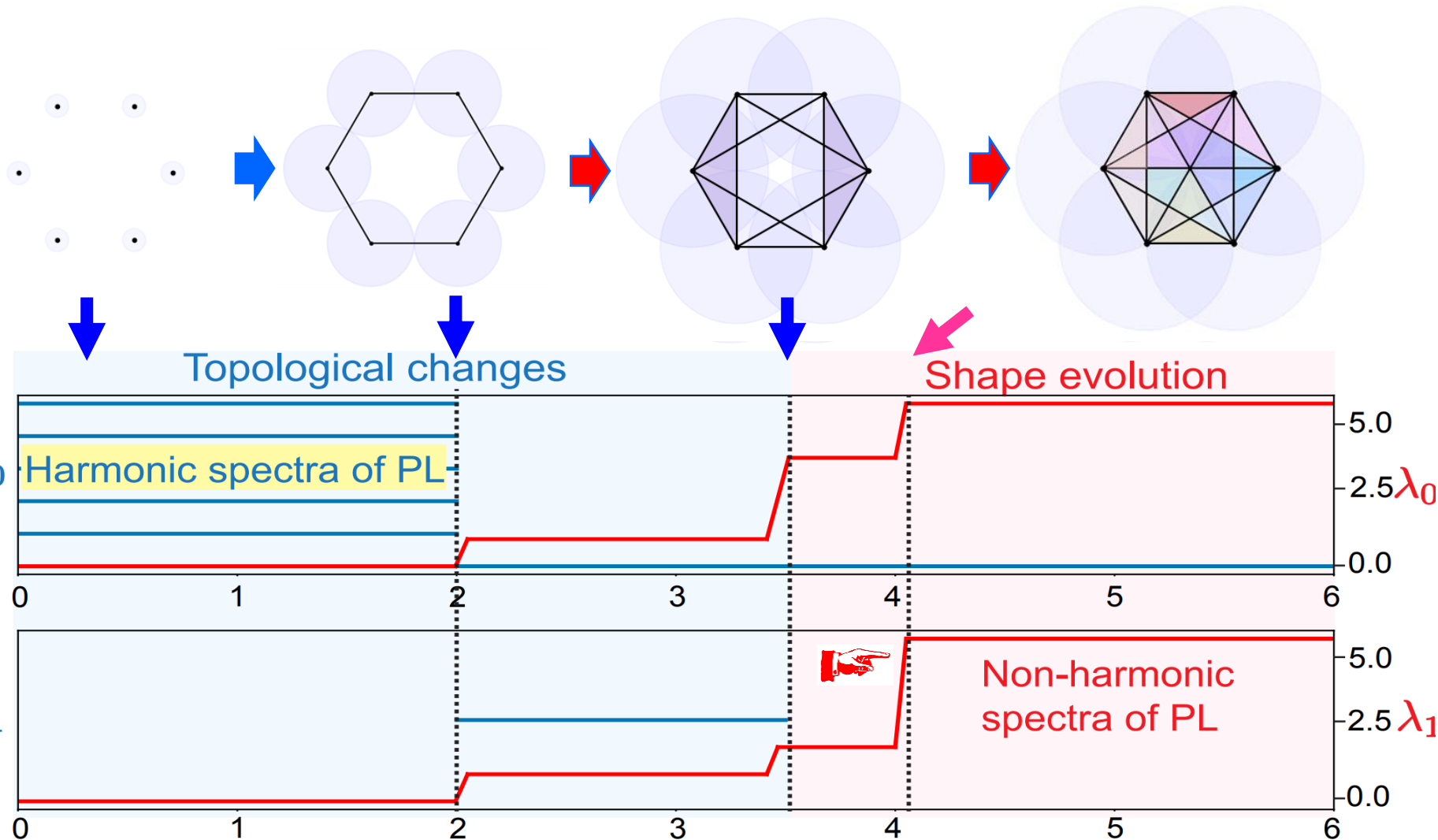
Persistent (Combinatorial) Laplacians



Rui Wang

$$\mathcal{L}_q^{t+p} = \mathcal{B}_{q+1}^{t+p} \left(\mathcal{B}_{q+1}^{t+p} \right)^T + \left(\mathcal{B}_q^{t+p} \right)^T \mathcal{B}_q^{t+p}$$

(Wang, Nguyen, Wei, 2019; Meng et al. 2021; Memoli et al. 2022; Liu and Wu 2023)



Alternative: Persistent Dirac by Maroulas and coworkers, Xia and coworkers

More in our toolbox for TDA



Evolutionary Homology

Zixuan Cang, Munch, Wei, *J. Appl. Comput. Topology*, 2020



Persistent sheaf Laplacians

Xiaoqi Wei, Wei, *under review*, 2021



Persistent Path Laplacians

Rui Wang, Wei, *Foundation of Data Science*, 2023



Persistent hypergraph Laplacians

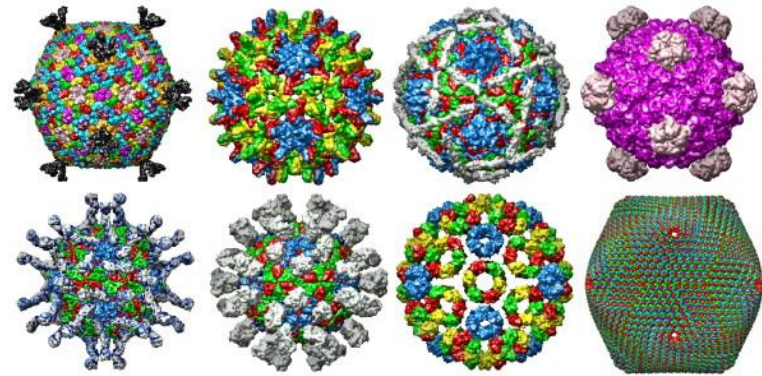
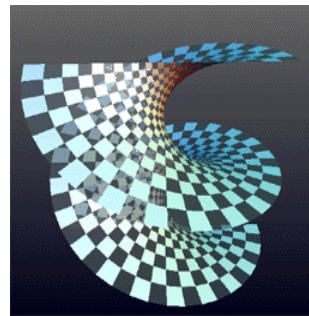
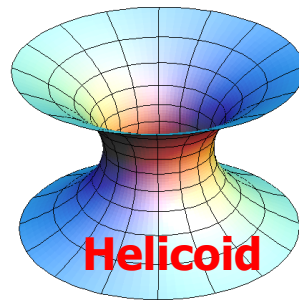
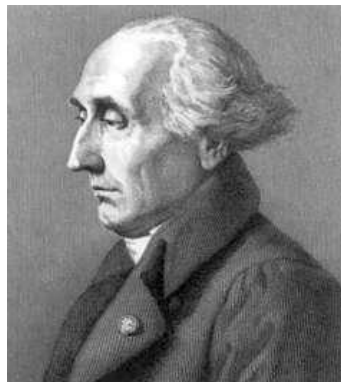
Dong Chen, Liu, Wu, Wei, 2023



Persistent hyperdigraph Laplacians

Dong Chen, Liu, Wu, Wei, 2023

Differential geometry

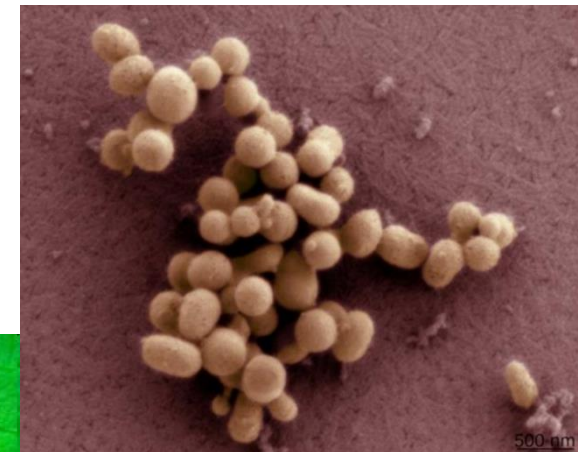
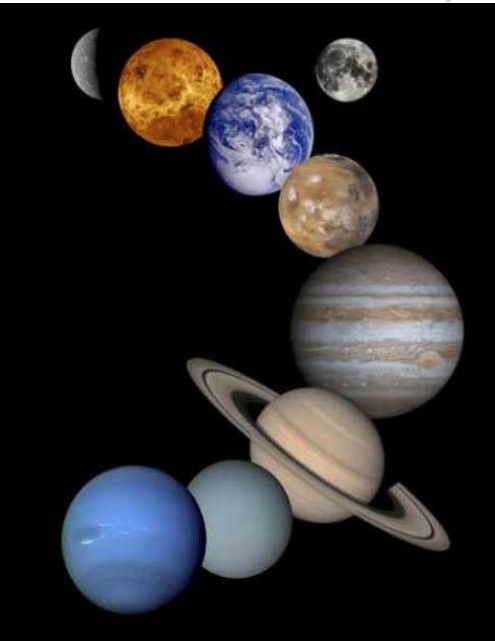


Viral morphology

Joseph L. Lagrange
(Italian
Mathematician,
January 25 1736 –
April 10, 1813)

Minimal Surfaces

A way to minimize energy
and maximize stability



Man-made life,
Mycoplasma
mycoides

Leonhard P. Euler
(Swiss Mathematician,
April 15, 1707 – Sept
18 1783)

Differential geometry based multiscale model

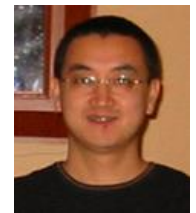
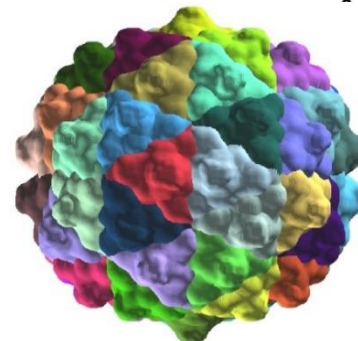
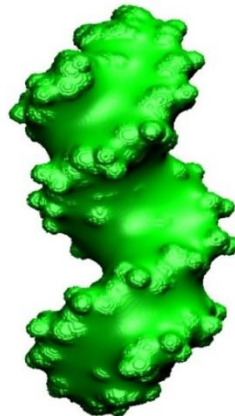
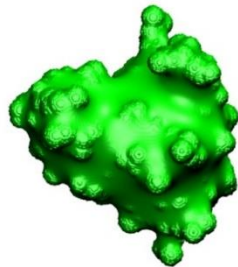
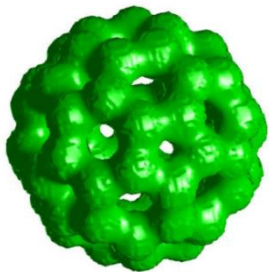
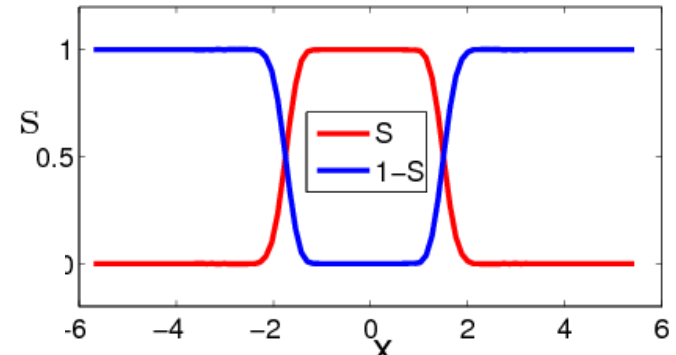
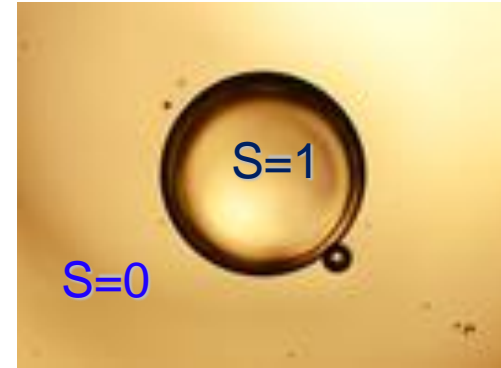
$$G = \int \gamma[\text{area}] dr \quad \text{area} = |\nabla S|$$

where G is the surface energy, γ (gamma) is the surface tension, and S is a surface characteristic function:

Generalized Laplace-Beltrami flow:

$$\frac{\partial S}{\partial t} = |\nabla S| \left[\nabla \cdot \frac{\gamma \nabla S}{|\nabla S|} \right]$$

Mean curvature

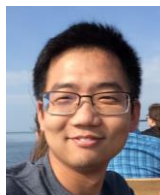


Shan Zhao

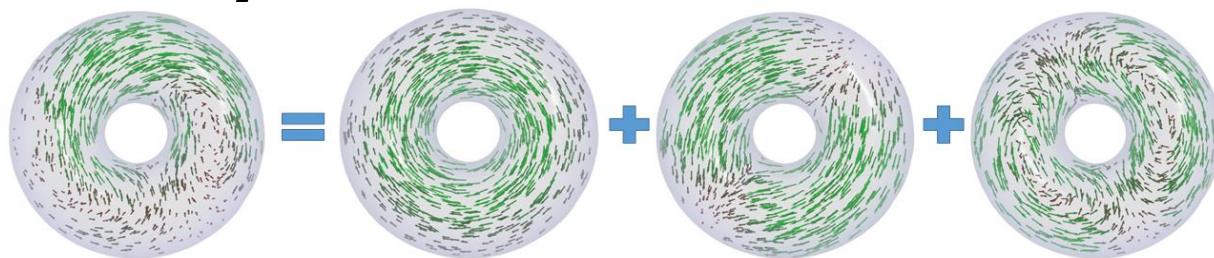
(Bates, Wei, Zhao, 2006; JCC,2008; Zhao, Cang, Tong & Wei, Bioinformatics 2018)

De Rham-Hodge theory and discrete exterior calculus

Hodge decomposition:

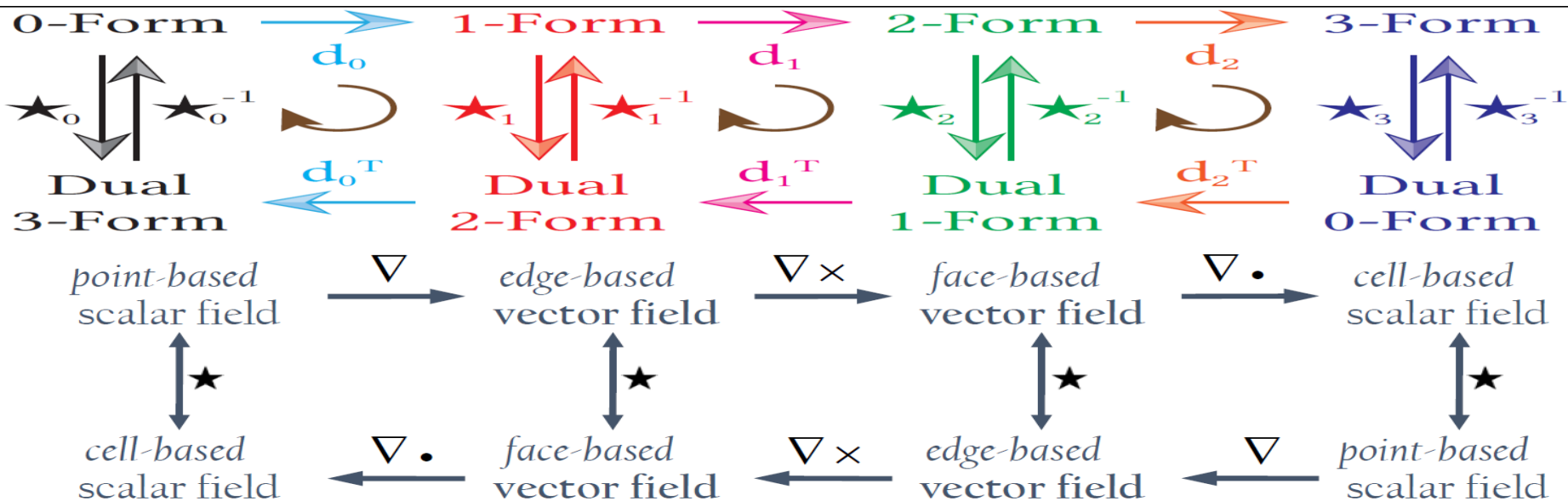
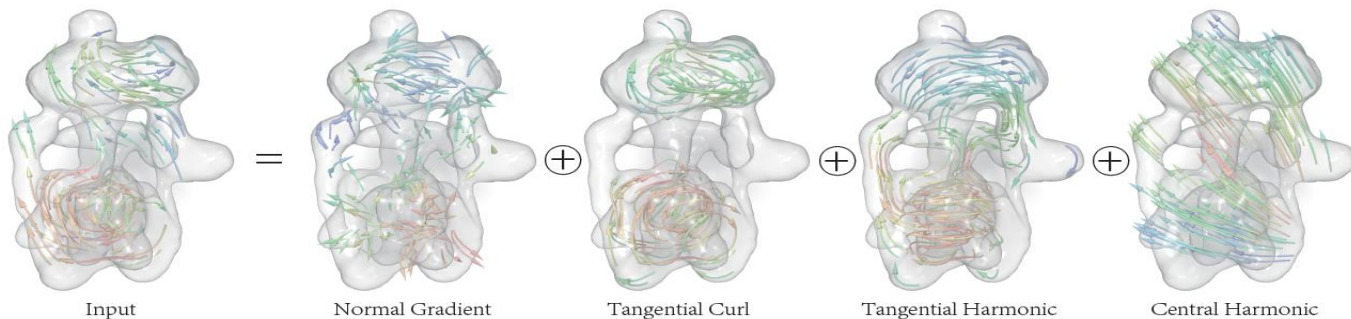


(Zhao, Wang, Chen, Tong & Wei, BMB, 2020)

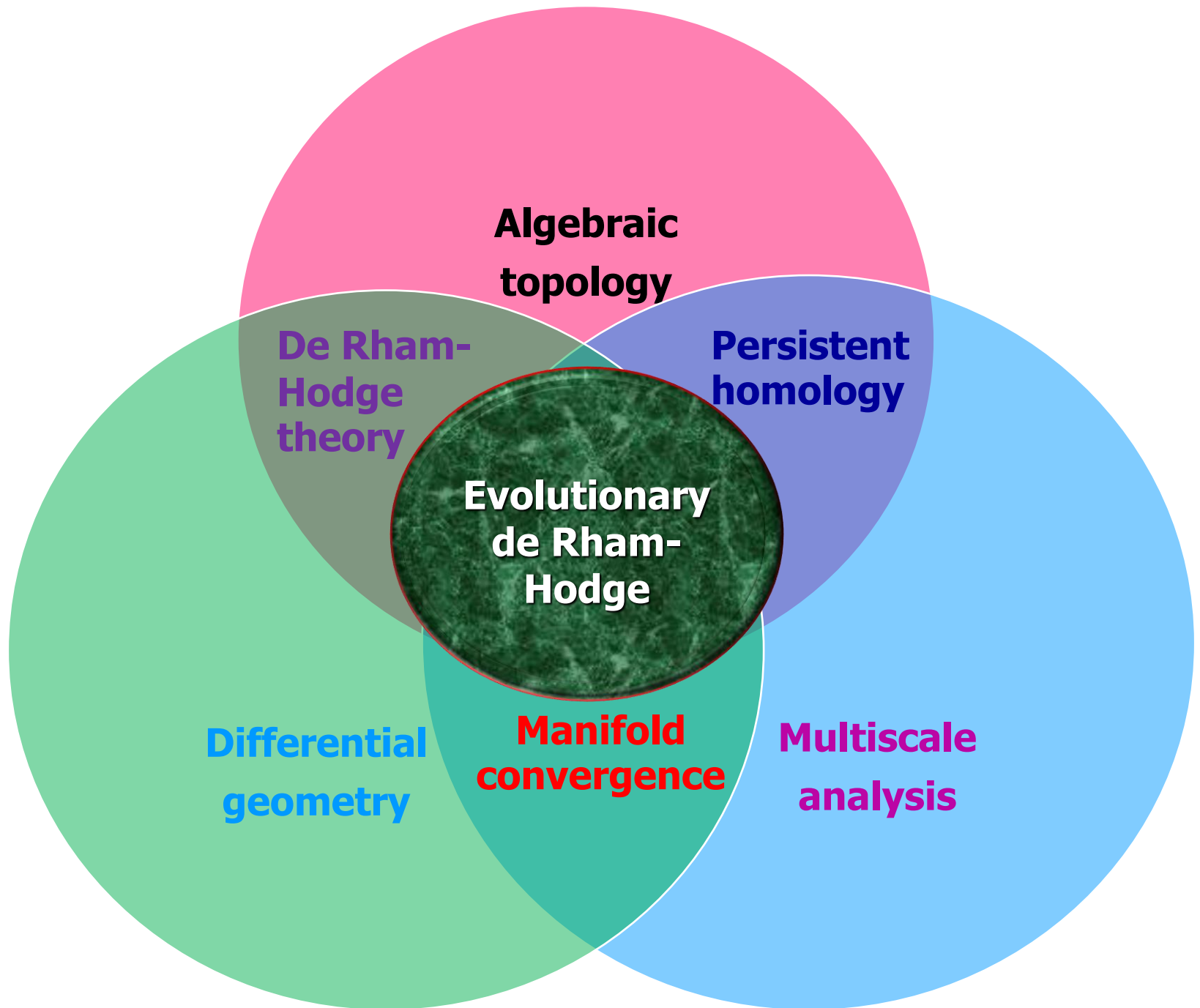


A vector field = Harmonic + curl-free + divergent-free

Cryo-EM data:

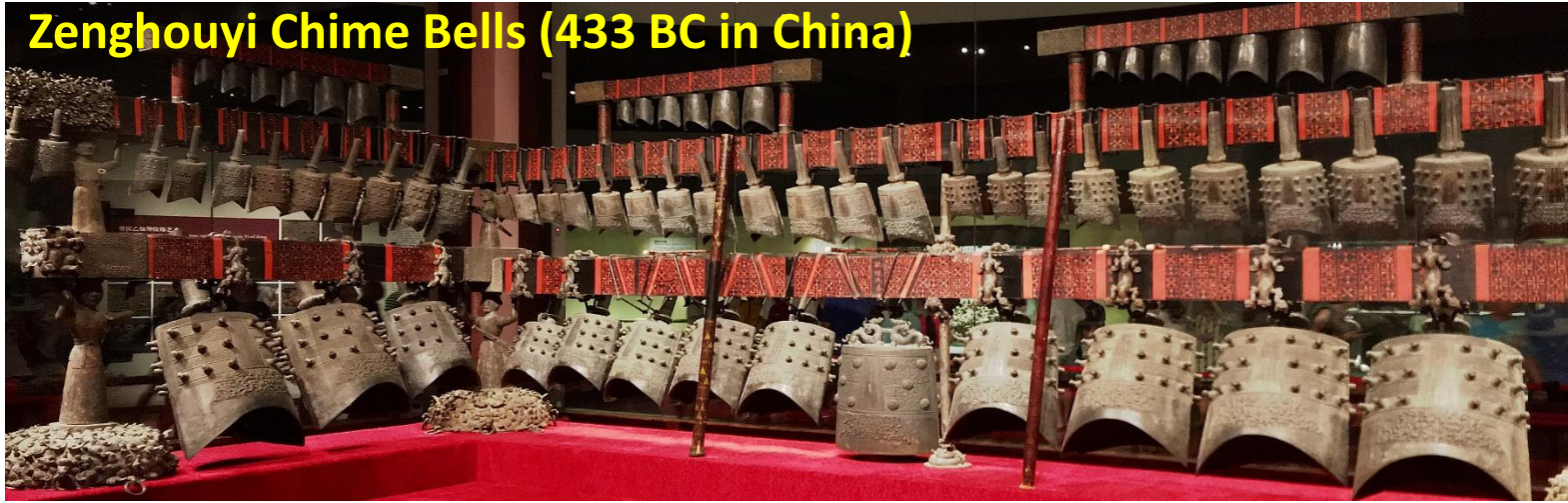


(Douglas Arnold, M Desbrun, AN Hirani, ...)



Evolutionary de Rham-Hodge

Zenghouyi Chime Bells (433 BC in China)



Manifold filtration

$$M_0 \xrightarrow{\mathfrak{I}_{0,1}} M_1 \xrightarrow{\mathfrak{I}_{1,2}} M_2 \xrightarrow{\mathfrak{I}_{2,3}} \dots \xrightarrow{\mathfrak{I}_{n-1,n}} M_n \xrightarrow{\mathfrak{I}_{n,n+1}} M$$

Filtration-induced de Rham complexes:

$$\begin{array}{ccccccc}
 \Omega_n^0(M_0) & \xrightarrow{d^0} & \Omega_n^1(M_0) & \xrightarrow{d^1} & \Omega_n^2(M_0) & \xrightarrow{d^2} & \Omega_n^3(M_0) \\
 \downarrow \mathfrak{E}_{0,1} & & \downarrow \mathfrak{E}_{0,1} & & \downarrow \mathfrak{E}_{0,1} & & \downarrow \mathfrak{E}_{0,1} \\
 \Omega_n^0(M_1) & \xrightarrow{d^0} & \Omega_n^1(M_1) & \xrightarrow{d^1} & \Omega_n^2(M_1) & \xrightarrow{d^2} & \Omega_n^3(M_1) \\
 \downarrow \mathfrak{E}_{1,1} & & \downarrow \mathfrak{E}_{1,1} & & \downarrow \mathfrak{E}_{1,1} & & \downarrow \mathfrak{E}_{1,1} \\
 \Omega_n^0(M_2) & \xrightarrow{d^0} & \Omega_n^1(M_2) & \xrightarrow{d^1} & \Omega_n^2(M_2) & \xrightarrow{d^2} & \Omega_n^3(M_2) \\
 \downarrow \mathfrak{E}_{2,1} & & \downarrow \mathfrak{E}_{2,1} & & \downarrow \mathfrak{E}_{2,1} & & \downarrow \mathfrak{E}_{2,1} \\
 \dots & & \dots & & \dots & & \dots
 \end{array}$$



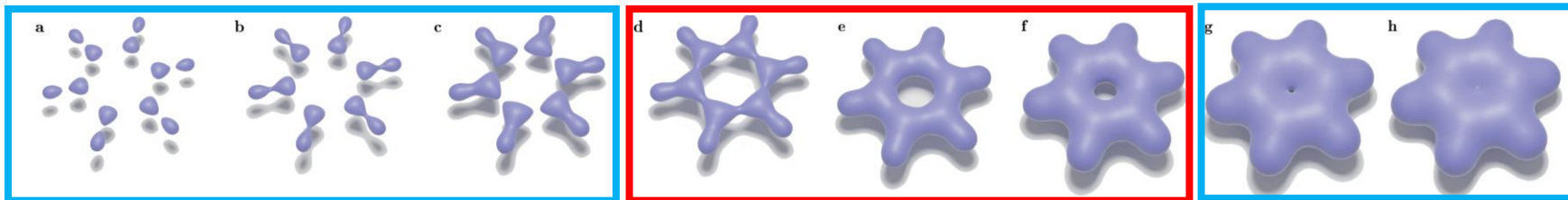
(Chen, Zhao, Tong & Wei, DCDS-B, 2020)

Evolutionary de Rham-Hodge Laplacians



$$\Delta_k^{l,p} = \partial_{k+1}^l d_k^l + d_{k-1}^{l+p} \partial_k^{l+p}$$

Manifold filtration:

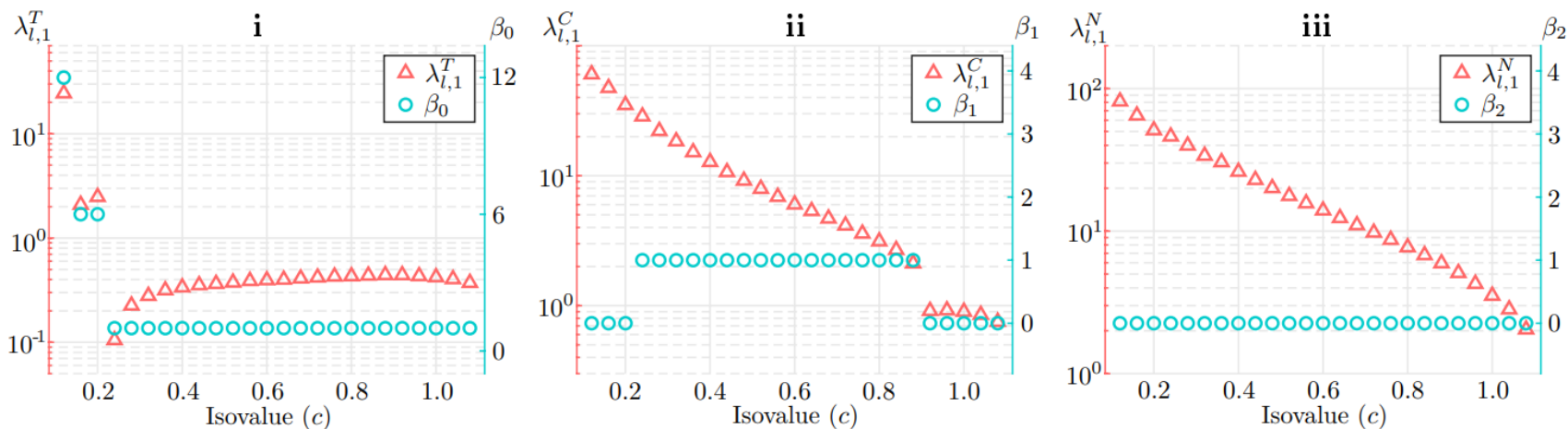


Topological persistence

Homotopic shape evolution

Topological persistence

Discontinuous harmonic (topological) and continuous non-harmonic spectra



(Chen, Zhao, Tong & Wei, DCDS-B, 2020)

Mathematical learning algorithms

Logistic regression

Support vector machine

Random forest

Ensemble methods

Transfer learning

Active learning

Deep neural network

Convolutional neural network

Nature language processing

Recurrent neural network

Long-short term memory

Graph neural network

Generative AI

ChatGPT

Autoencoder

Transformer

Manifold learning

Graph learning

Geometric learning

PCA

UMAP

t-SNE

Correlated clustering and projection

Topological deep learning

Multiscale Laplacian learning

D3R Grand Challenge 4 (2018-2019)



Our performance in D3R Grand Challenges, worldwide competitions in computer-aided drug design organized by NIH, 2016-2019.

Pose Predictions

BACE Stage 1A

Pose Predictions (Partials)  

BACE Stage 1B

Pose Prediction (Partials)  

Affinity Predictions

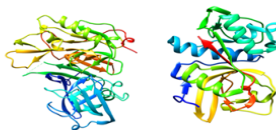
Cathepsin Stage 1

Combined Ligand and Structure Based Scoring   

Ligand Based Scoring (No participation)

Structure Based Scoring   

Free Energy Set   



BACE Stage 1

Combined Ligand and Structure (No participation)

Ligand Based Scoring (Partials) (No participation)

Structure Based Scoring (Partials) (No participation)

Free Energy Set (No participation)

BACE Stage 2

Combined Ligand and Structure

Ligand Based Scoring (No participation)

Structure Based Scoring (Partials)

Free Energy Set  

D3R Grand Challenge 3 (2017-2018)

(Nguyen et al, JCAMD, 2018)

Pose Prediction

Cathepsin Stage 1A

Pose Predictions (partials)

Affinity Rankings excluding Kds > 10 μM

Cathepsin Stage 1

Scoring (partials)

Free Energy Set

VEGFR2

Scoring (partials)

JAK2 SC3

Scoring

Free Energy Set   

Active / Inactive Classification

VEGFR2

Scoring (partials)

JAK2 SC3

Scoring

Free Energy Set   

Affinity Rankings for Cocrystallized Ligands

Cathepsin Stage 1

Scoring (partials)

Free Energy Set  

Cathepsin Stage 1B

Pose Prediction

Affinity Rankings excluding Kds > 10 μM

Cathepsin Stage 2

Scoring (partials)

Free Energy Set

JAK2 SC2

Scoring (partials)

TIE2

Scoring  

Free Energy Set 2   

JAK2 SC2

Scoring (partials)

TIE2

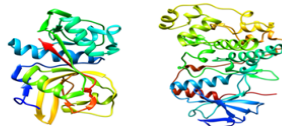
Scoring (partials)

Free Energy Set 1   

Cathepsin Stage 2

Scoring (partials)

Free Energy Set   



p38-α

Scoring

ABL1

Scoring (partials)   

p38-α

Scoring (partials)

ABL1

Scoring (partials)



D Nguyen



Zixuan Cang



Kaifu Gao

D3R Grand Challenge 2 (2016-2017)

Given: Farnesoid X receptor (FXR) and 102 ligands

Tasks: Dock 102 ligands to FXR, and predict their poses, binding free energies and energy ranking

Stage 1

Pose Predictions (partials)

Scoring (partials)

Free Energy Set 1 (partials)

Free Energy Set 2 (partials)

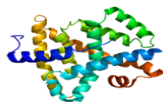
Stage 2

Scoring (partials)

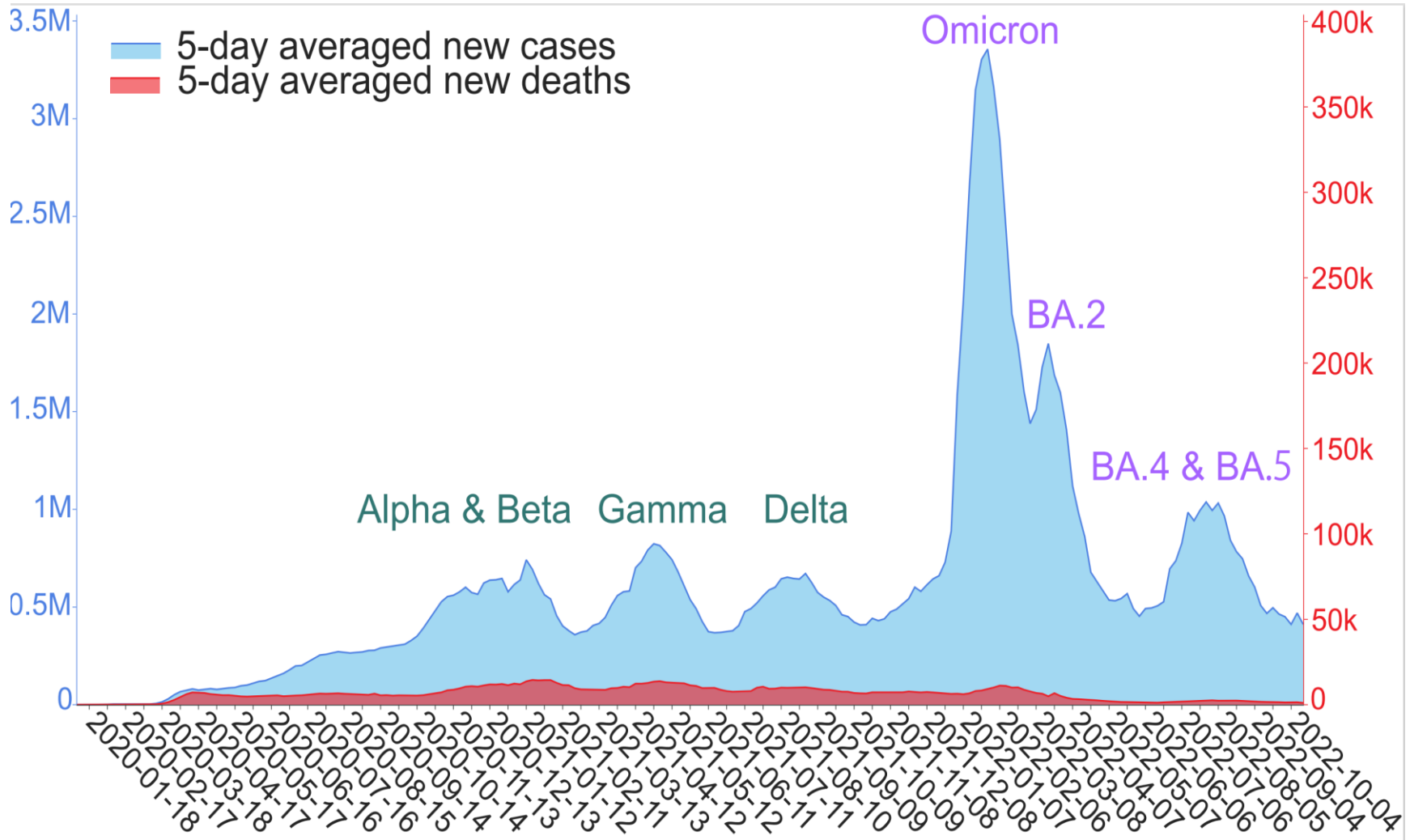
Free Energy Set 1 (partials)

Free Energy Set 2 (partials)



Evolution of SARS-CoV-2 variants



What are the evolutionary mechanisms?

Mutation Tracker

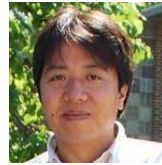
https://users.math.msu.edu/users/weig/SARS-CoV-2_Mutation_Tracker.html



Rui Wang



Y. Hozumi



Dr. CC Yin

29304 Single Mutations in 3658198 hCoV-19 Genomes

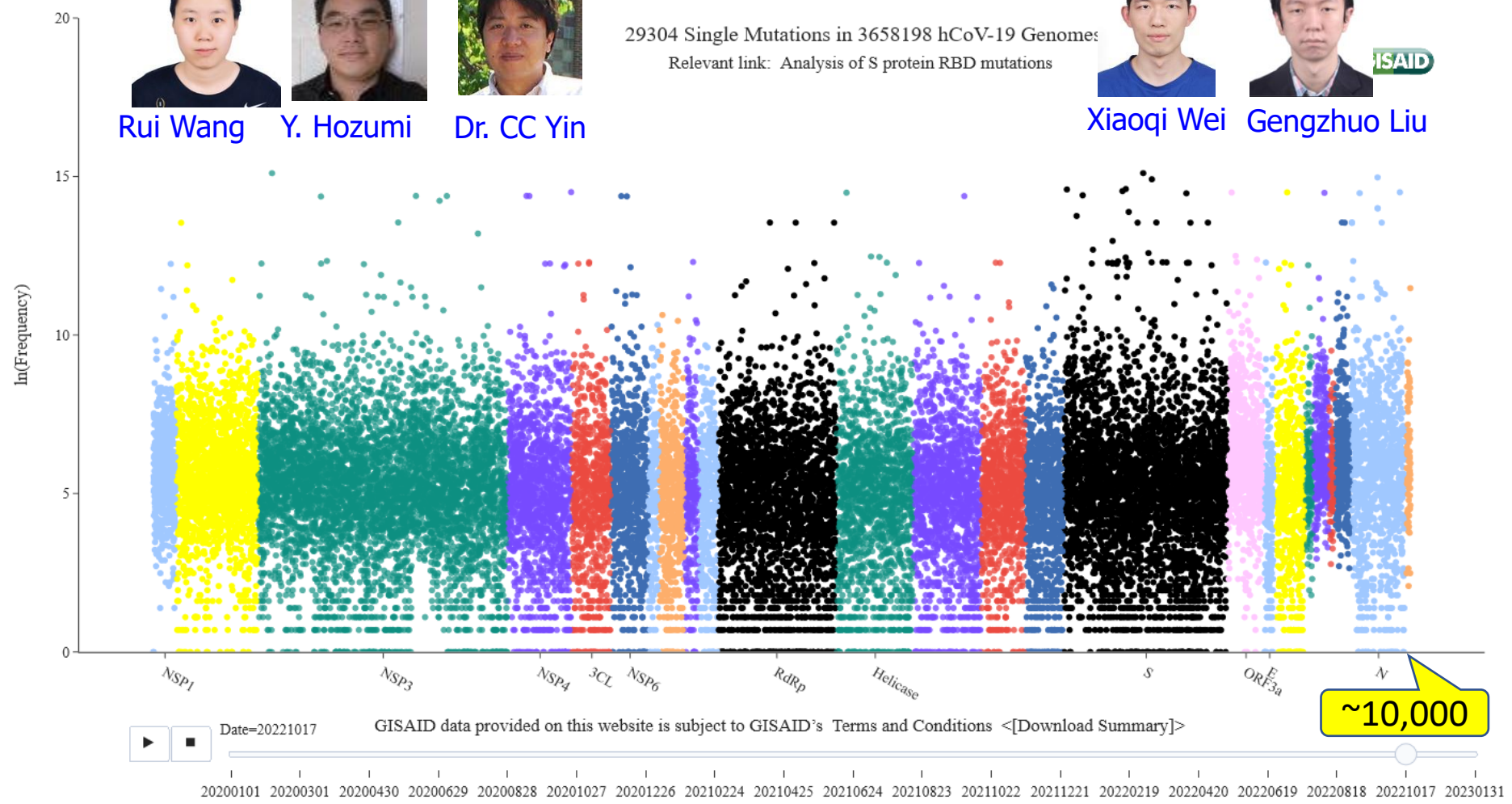
Relevant link: [Analysis of S protein RBD mutations](#)



Xiaoqi Wei



Gengzhuo Liu



What governs SARS-CoV-2 transmission and evolution?

Competing mechanisms of SARS-CoV mutations

Molecular scale

Random genetic shifts

Replication errors

Transcription errors

Translation errors

Recombination

Viral proofreading

Organism scale

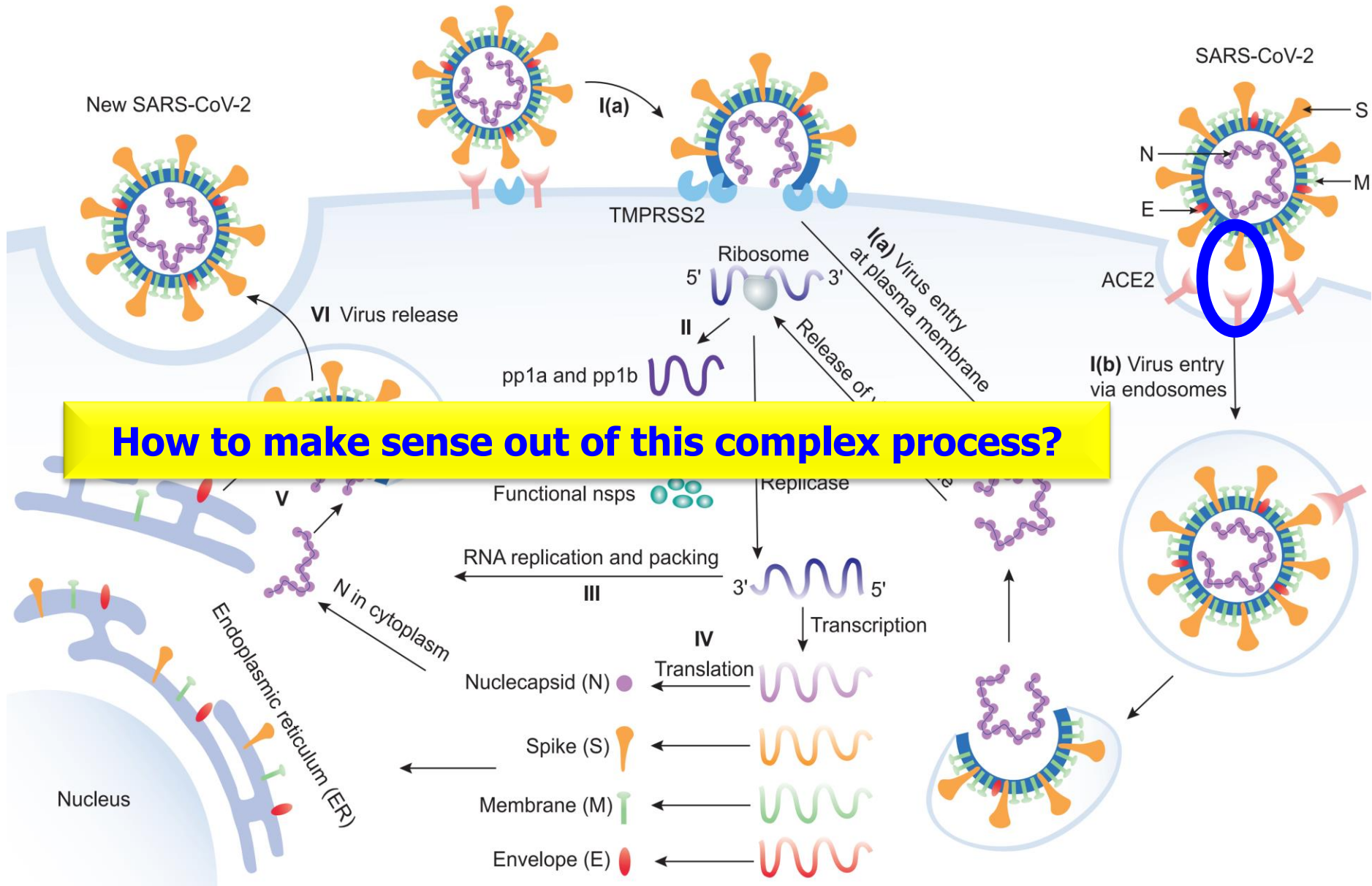
Host gene editing

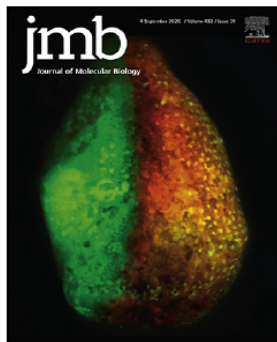
Recombination

Population scale

Natural selection

Life cycle of SARS-CoV-2 in a host cell





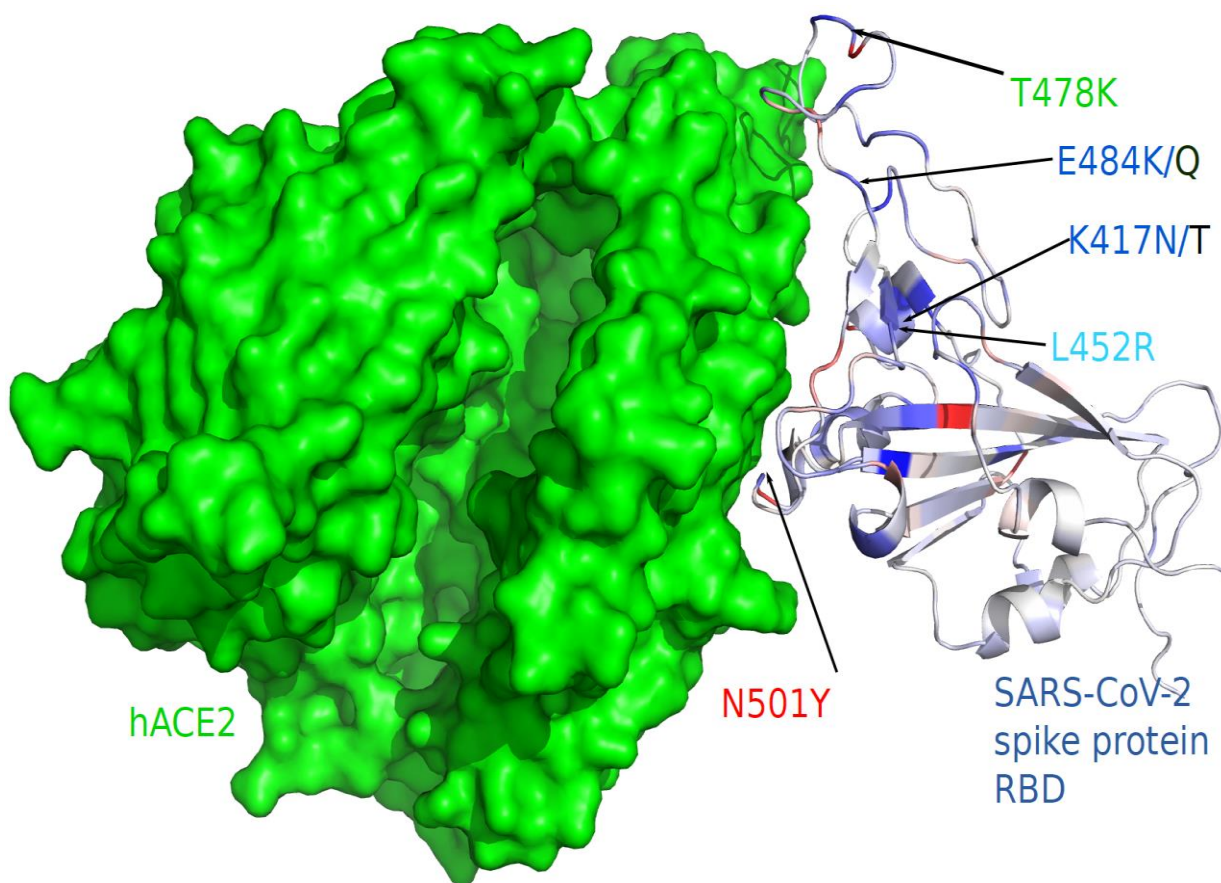
Mutations Strengthened SARS-CoV-2 Infectivity



Dr Jiahui Chen

We predicted prevailing SARS-CoV-2 variants to occur at residues **452** and **501**

Jiahui Chen¹, Rui Wang¹, Menglun Wang¹ and Guo-Wei Wei^{1,2,3}



Alpha: **N501Y**

Beta: K417N, E484K, **N501Y**

Gamma: K417T, E484K, **N501Y**

Delta: **L452R**, T478K

Epsilon: **L452R**

Theta: E484K, **N501Y**

Kappa: **L452R**, E484Q

Lambda: **L452Q**, F490S

Mu: R346K, E484K, **N501Y**

Omicron: G339D, S371L, S373P, S375F, K417N, N440K, G446S, S477N, T478K, E484A, Q493R, G496S, Q498R, **N501Y**, Y505H;

BA.2.12.1: Omicron + **L452Q**;

BA.4/BA.5: Omicron + **L452R**

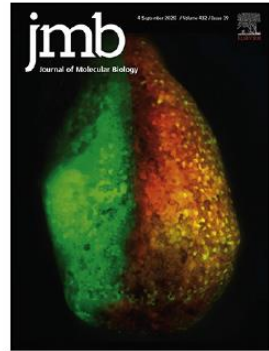
We discovered the mechanism of viral transmission and evolution

89) of all mutations on the RBD, which potentially increases the complexity of antiviral drug and vaccine development. This global analysis indicates that mutations on the RBD strengthen the binding of S protein and ACE2, leading to more infectious SARS-CoV-2.

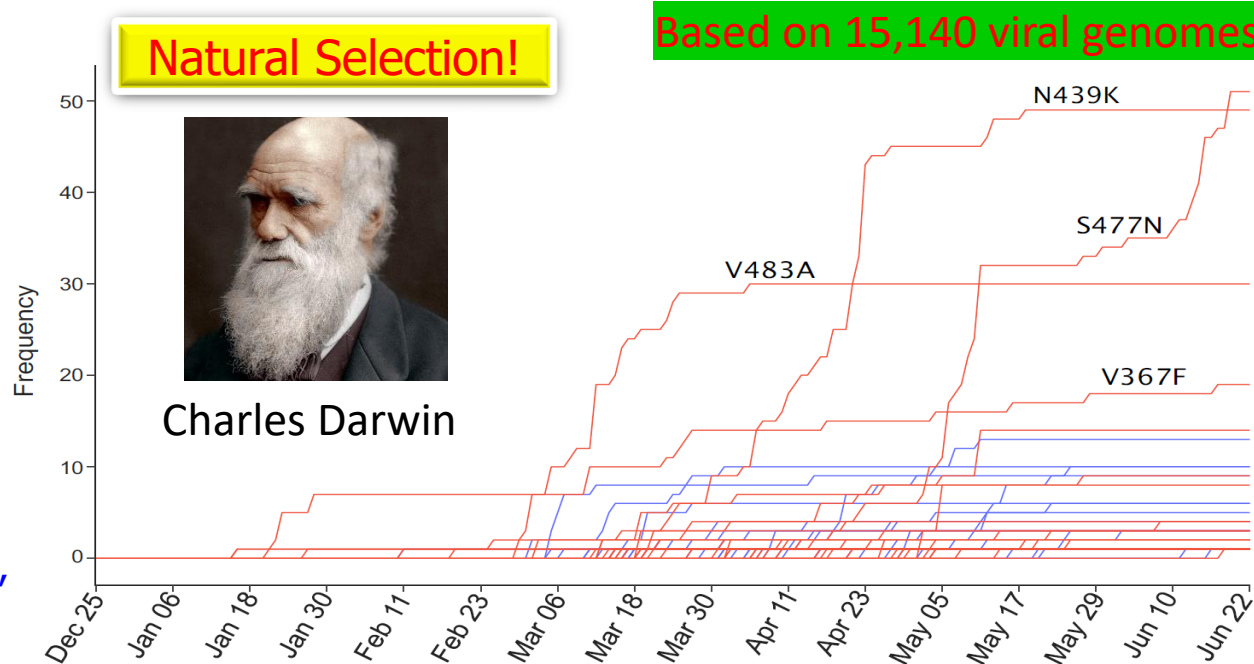
We hypothesize that natural selection favors those mutations that enhance the viral transmission and if our predictions are correct, the predicted infectivity strengthening mutations will outpace predicted infectivity weakening mutations over time. Figure 3 illustrates the increase in the frequency of each

strengthening mutations occurred. It is interesting to note that overall, infectivity-strengthening mutations grow faster than infectivity-weakening mutations, which also reveals that SARS-CoV-2 subtypes having infectivity-strengthening mutations are able to infect more people. Specifically, frequencies of S477N, N439K, V483A, and V367F are higher than those of other mutations, indicating these mutations have a stronger transmission capacity.

The SARS-CoV-2 genotypes are clustered into six clusters or subtypes based on their single nucleotide



Chen, Wang, Wang,
Wei, JMB, 432, 5212,
July 2020



Dr Jiahui Chen



Rui Wang

Figure 3. The time evolution of 89 SARS-CoV-2 S protein RBD mutations. The red lines represent the mutations that strengthen the infectivity of SARS-CoV-2 (i.e., $\Delta\Delta G$ is positive), and the blue lines represent the mutations that weaken the infectivity of SARS-CoV-2 (i.e., $\Delta\Delta G$ is negative). Many mutations overlap their trajectories. Here, the collection date of each genome sequence that deposited in GISAID is applied.

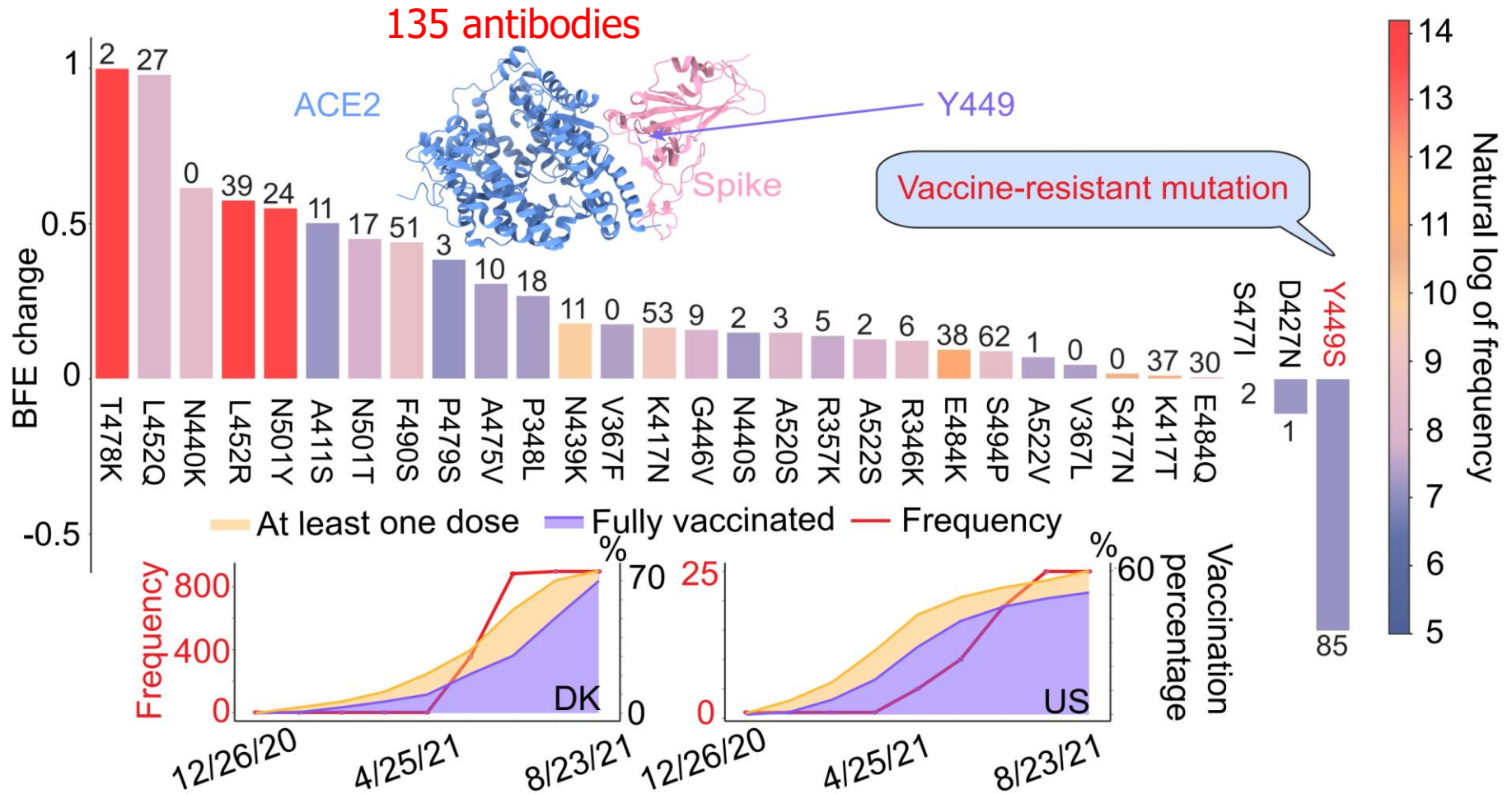
Vaccine-breakthrough mutations

By genotyping 2,298,349 viral genomes isolated from patients

Wang, Chen, and Wei, J. Phys. Chem. Letter, 12. 11850-11857 2021



Rui Wang



Evolution mechanisms --- Natural selection via two complementary transmission pathways: Infectivity strengthening and vaccine breakthrough

Omicron BA.2 (B.1.1.529.2): high potential to becoming the next dominating variant

Jiahui Chen¹ and Guo-Wei Wei^{1,3,4*}

¹ Department of Mathematics,
Michigan State University, MI 48824, USA.



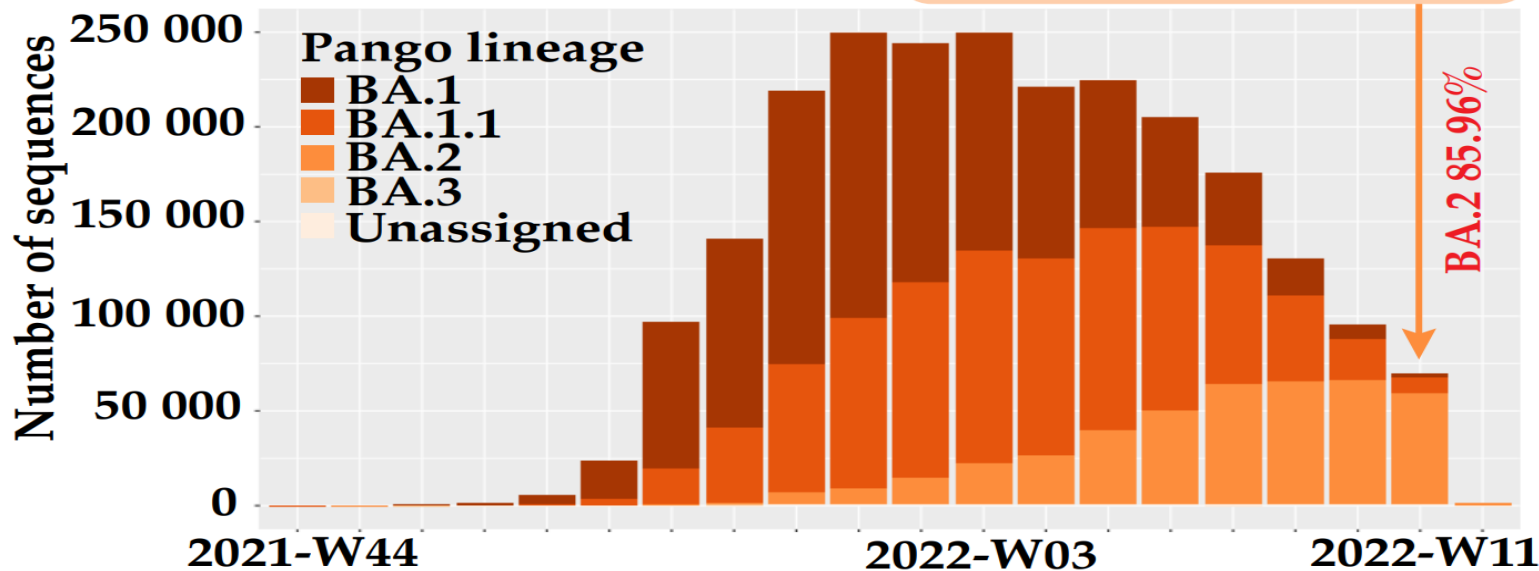
Dr Jiahui Chen



World Health Organization

COVID-19 Weekly Epidemiological Update
Edition 84, published 22 March 2022

On 2/10/2022, we predicted that BA.2 will become the dominant variant. This became the reality in later March according to WHO



This was confirmed by WHO on March 22, 2022!
All other predictions were confirmed within 50 days

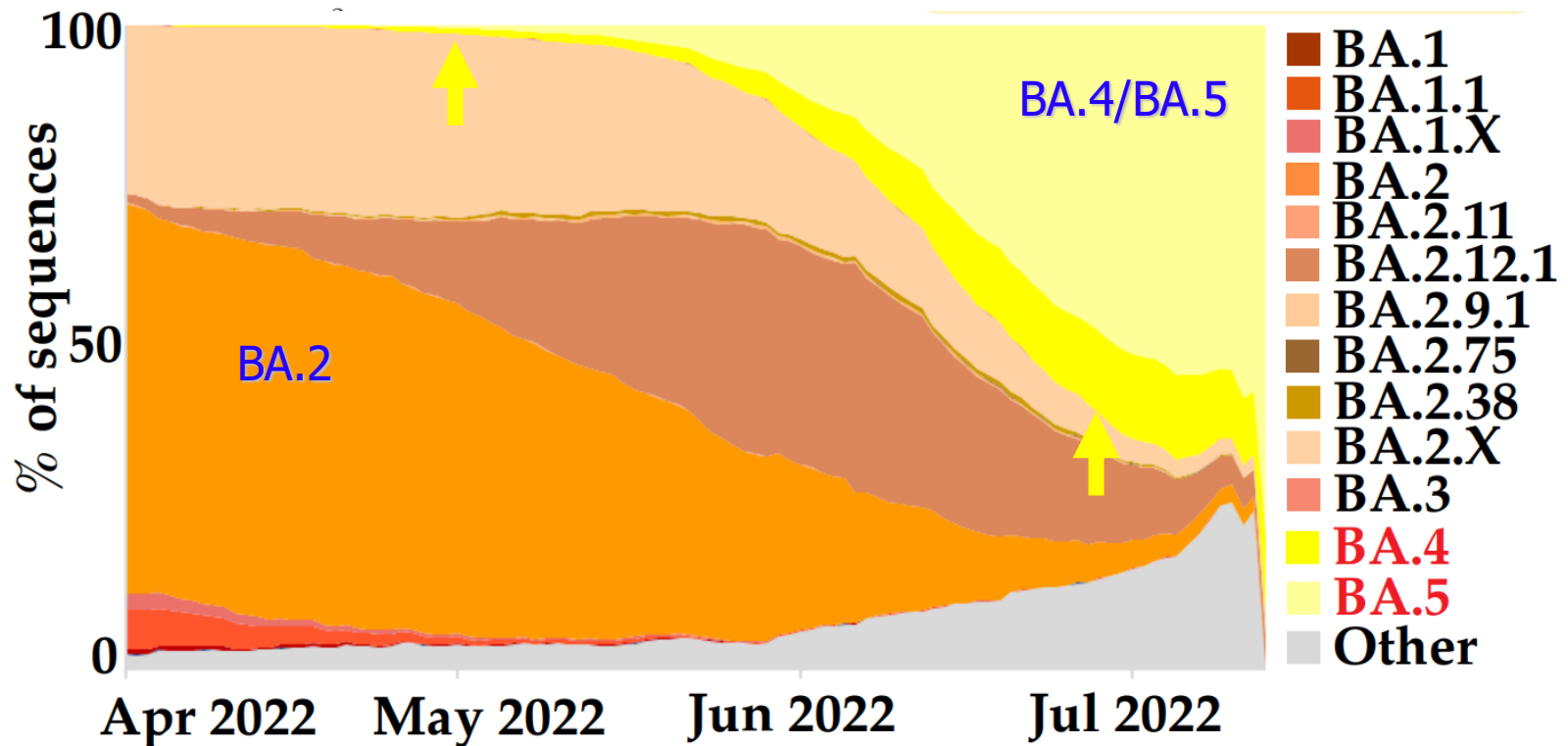
Persistent Laplacian projected Omicron BA.4 and BA.5 to become new dominating variants

Jiahui Chen¹, Yuchi Qiu¹, Rui Wang¹, and Guo-Wei Wei^{1,2,3*}

¹ Department of Mathematics,
Michigan State University, MI 48824, USA.
East Lansing, MI 48823 USA.



Dr Jiahui Chen



**This was confirmed by WHO in early July
(WHO weekly update release number 101)**

Characterizing Musical Sounds with Topological Data Analysis

By Guo-Wei Wei shape based

SIAM NEWS BLOG

 Research | August 09, 2022

 Print

Topological Artificial Intelligence Forecasting of Future Dominant Viral Variants

By Guo-Wei Wei

SIAM NEWS MAY 2020

 Research | May 01, 2020

 Print

Math and AI-based Repositioning of Existing Drugs for COVID-19

By Duc D. Nguyen and Guo-Wei Wei

SIAM NEWS DECEMBER 2017

 Research | December 01, 2017

Persistent Homology Analysis of Biomolecular Data

By Guo-Wei Wei

Over one hundred
of news and media
coverages

SIAM NEWS BLOG

 Research | June 06, 2023

 Print

Mathematics-assisted Directed Evolution and Protein Engineering

By Yuchi Qiu and Guo-Wei Wei

SIAM NEWS BLOG

 Research | December 18, 2017

Mathematics at a Historic Transition in Biology

By Guo-Wei Wei

SIAM NEWS SEPTEMBER 2016

 Get Involved | September 01, 2016

Mathematical Molecular Bioscience and Biophysics

A Recurring Theme at the SIAM Conference on the Life Sciences

By Guo-Wei Wei

Algebraic graph

Geometric topology

Differential topology

Algebraic topology

Geometric Algebra

Topological graph

Number theory

Statistics

Vision:
The last frontier of science and technology is biological science

Algebraic geometry

Probability

The last frontier of biological science is mathematics

Differential geometry

Differential equation

Symplectic geometry

Numerical analysis

Multiscale analysis

Harmonic analysis

Real analysis

Stochastic analysis

